Journal of Molecular Graphics and Modelling 30 (2011) 90–99

Contents lists available at ScienceDirect

Journal of Molecular Graphics and Modelling

journal homepage: www.elsevier.com/locate/JMGM

The design and inhibitory profile of new benzimidazole derivatives against triosephosphate isomerase from *Trypanosoma cruzi*: A problem of residue motility☆

Antonio Romo-Mancillas[a], Alfredo Téllez-Valencia[b], Lilián Yépez-Mulia[c], Francisco Hernández-Luis[a], Alicia Hernández-Campos[a], Rafael Castillo[a,*]

[a] Facultad de Química, Departamento de Farmacia, Universidad Nacional Autónoma de México, México DF 04510, Mexico
[b] Facultad de Medicina, Centro de Investigaciones en Alimentos y Nutrición, Universidad Juárez del Estado de Durango, Durango 34000, Mexico
[c] Unidad de Investigación Médica en Enfermedades Infecciosas y Parasitarias, IMSS, México DF, Mexico

ARTICLE INFO

Article history:
Received 10 February 2011
Received in revised form 18 June 2011
Accepted 21 June 2011
Available online 29 June 2011

Keywords:
Docking
Triosephosphate isomerase
Benzimidazole
Homodimeric interface

ABSTRACT

To develop a new set of compounds with inhibitory activity against the triosephosphate isomerase of *Trypanosoma cruzi* (TcTIM), a group of benzimidazole derivatives was studied using four different docking procedures. These docking procedures differ in the number and type of mobile residues considered in the analysis. As a result of this methodology, a clustered analysis of plausible candidate structures was produced. A different set of previously synthesized compounds was used to validate this analysis. The validation showed that the best results correspond to the docking procedure in which the residues near the hydrophobic pocket of the protein's interface were considered mobile. A binding site for the best candidates was identified. Residues Tyr103, Glu105 and Lys113, among others, are important for the binding of this kind of compound. Residue Tyr103 is different in the human TIM, thus establishing a key feature for the future design of selective inhibitors.

1. Introduction

According to the World Health Organization [1], American trypanosomiasis or Chagas disease affects approximately 28 million people in the American continent, particularly in Latin-American countries. Endemic to this continent, Chagas disease is caused by infection of the flagellated protozoan *Trypanosoma cruzi*. Mild symptoms are common to all infections in the early stages of the disease. However, if left untreated this infection can cause severe organ dysfunction and death in 20–30% of affected individuals several years after infection. Thus, life expectancy for these individuals is diminished by almost 15 years. This disease is considered incurable, without effective treatment, and is classified as "neglected" for economic reasons. Still, some research groups have focused on studying the parasite's metabolic pathways to identify possible drug targets [2]. Among the plethora of biological targets, there has been considerable attention given to block the parasite's only energy supply: the glycolytic pathway [3,4].

Among other enzymes in this metabolic pathway, triosephosphate isomerase (TIM) has been identified as an important enzyme that acts at a crucial step [3]. This homodimeric enzyme catalyzes the interconversion of dihydroxyacetone-phosphate (DHAP) to glyceraldehyde-3-phosphate (G3P) [5]. TIM is present in both human (HsTIM) and *T. cruzi* (TcTIM) cells, and it contains a highly conserved catalytic site. These facts make difficult to design drugs that are focused on this site. Therefore, to inhibit this enzyme a putative "allosteric" control site, which is extremely hydrophobic and is located at the homodimeric interface, has been proposed [6,7]. The conforming residues vary from species to species. For example, this hydrophobic site in TcTIM is formed by aromatic residues, whereas aliphatic and aromatic residues in HsTIM [8]. Several efforts have been made to find a selective inhibitor to TcTIM, among these brevifolin derivatives extracted from natural products [9], heterocyclic systems like phenazine dioxides, thiadiazines and thiazoles among others found by high-throughput screening [10], and a group of amphiphilic benzothiazole derivatives [8,11,12] that have been extensively studied *in silico* [13–16]. It could be extracted from these works that the interface of TcTIM has affinity for molecules that are mostly aromatic heterocyclic systems.

Our research group has synthesized a large number of benzimidazole derivatives with antiparasitic activity [17–19]. Some of these compounds present activity, ranging from poor to mild, as TcTIM inhibitors (see below). Since these benzimidazole derivatives act as inhibitors, broadening the spectra of scaffolds that could bind to this enzyme, a subsequent task would be to identify the

☆ Taken in part from the PhD thesis of Antonio Romo-Mancillas.

* Corresponding author. Tel.: +52 5556225287; fax: +52 5556225329.
E-mail address: rafaelc@servidor.unam.mx (R. Castillo).

1093-3263/$ – see front matter © 2011 Elsevier Inc. All rights reserved.
doi:10.1016/j.jmgm.2011.06.009

Table 1
Compounds used for this study.

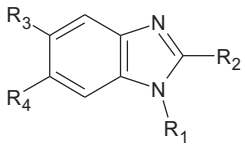

Compound	R_1	R_2	R_3	R_4[a]	Percent TcTIM inhibition at 100 μM	Compound	R_1	R_2	R_3	R_4[a]	Percent TcTIM inhibition at 100 μM
1	CH_3	CH_3	H	NTAC	30	**19**	CH_3	CF_3	TAC	Cl	0
2	CH_3	SCH_3	H	NTAC	10	**20**	CH_3	CF_3	NTAC	Cl	0
3	CH_3	SCH_3	Cl	TAC	7	**21**	CH_3	CF_3	Cl	TAC	0
4	CH_3	SCH_3	Cl	NTAC	29	**22**	CH_3	CF_3	Cl	NTAC	0
5	H	CH_3	NTAC	H	30	**23**	H	SCH_3	Nph	Cl	13
6	H	SCH_3	TAC	Cl	8	**24**	H	MCA	Nph	Cl	60
7	CH_3	SCH_3	TAC	Cl	40	**25**	CH_3	CF_3	Cl	Nph	10
8	CH_3	SCH_3	NTAC	Cl	50	**26**	H	CF_3	Nph	Cl	19
9	H	SCH_3	NTAC	Cl	30	**27**	H	MCA	PhS	H	48
10	H	CH_3	NTAC	Cl	6	**28**	H	H	NFCZ	H	5
11	H	CF_3	TAC	H	35	**29**	H	CH_3	NFCZ	H	0
12	H	CF_3	NTAC	Cl	40	**30**	H	CF_3	NFCZ	H	0
13	H	CF_3	TAC	Cl	10	**31**	H	SCH_3	NFCZ	H	40
14	CH_3	CH_3	H	TAC	30	**32**	CH_3	H	NFCZ	H	0
15	CH_3	SCH_3	H	TAC	8	**33**	CH_3	CH_3	NFCZ	H	0
16	CH_3	CF_3	H	NTAC	0	**34**	CH_3	CF_3	NFCZ	H	3
17	CH_3	H	H	TAC	0	**35**	CH_3	SCH_3	NFCZ	H	0
18	CH_3	H	H	NTAC	0						

Compound **36**

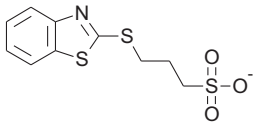

95% inh.[b] (250 μM, estimated 87% at 100 μM)

Compound **37**

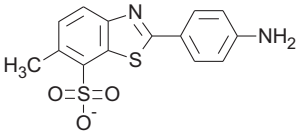

91% inh. (250 μM, estimated 84% at 100 μM)

Compound **38**

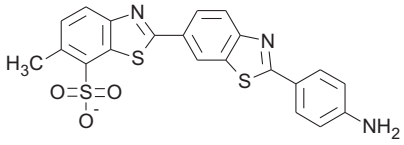

95% inh. (250 μM, estimated 87% at 100 μM)

Compound **A**

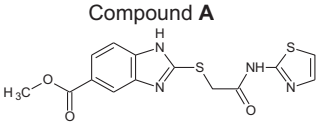

5% inh. (200 μM)

Compound **B**

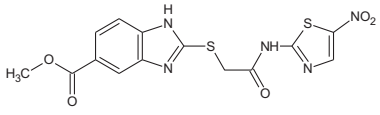

52% inh. (200 μM)

Compound **C**

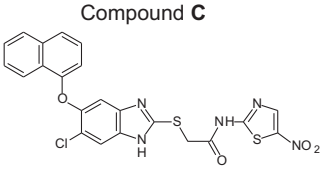

48% inh. (200 μM)

Compound **D**

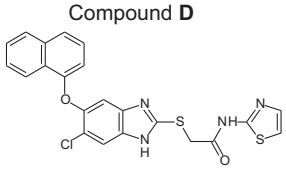

20% inh. (200 μM)

Compound **E**

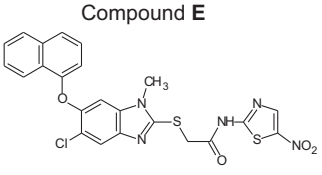

33% inh. (200 μM)

Compound **F**

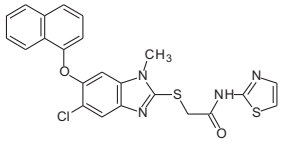

34% inh. (200 μM)

Compound **G**

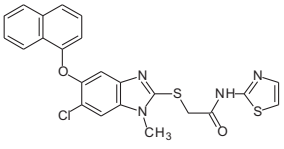

18% inh. (200 μM)

[a] NTAC: 5-nitro-1,3-thiazol-2-ylaminocarbonyl; TAC: 1,3-thiazol-2-ylaminocarbonyl; Nph: 1-Naphthyloxy; PhS: Phenylthio; MCA: Methoxycarbonylamino; NFCZ: *N*-(5-nitrofuran-2-yl)methylidenecarbohydrazido.

[b] inh: Percent TcTIM inhibition at the concentration marked in parentheses.

Table 2
Docking procedures.

Docking	I (Rigid)	II (Flexible)	III (Flexible)	IV (Flexible)	
Flexible residues	None	Tyr102	Glu78	Asn67	Tyr103
		Tyr103	Arg99	Ile69	Glu105
		Glu105	Tyr103	Glu78	Ile109
		Ile109	Glu105	Arg99	Glu112
		Lys113	Lys113	Tyr102	Lys113
Selection criteria for flexible residues	None	Residues within 5 Å from the conformations of the rigid–flexible docking (I)	Pocket finder SITE-ID®-SybyI® using a 3 Å protein depth search and 1 Å grid resolution	Residues within 5 Å from the interface center	

Table 3
Docking scores of compounds **1**–**38**.

Compound	Percent TcTIM inhibition at 100 μM	Binding energy (Δ*G*) (kcal/mol)				Compound	Percent TcTIM inhibition at 100 μM	Binding energy (Δ*G*) (kcal/mol)			
		I	II	III	IV			I	II	III	IV
1	30	−6.77	−24.63	−22.83	−33.78	**20**	48	−6.30	−24.39	−23.90	−32.01
2	10	−6.78	−24.86	−23.23	−29.85	**21**	0	−5.77	−22.51	−20.81	−29.58
3	7	−6.14	−23.07	−21.71	−28.50	**22**	0	−5.41	−23.96	−23.56	−30.34
4	29	−6.83	−22.93	−21.71	−31.00	**23**	0	−6.75	−24.37	−22.81	−30.04
5	30	−6.54	−24.11	−22.27	−30.75	**24**	0	−5.55	−21.73	−24.04	−31.40
6	8	−5.81	−24.04	−21.76	−31.35	**25**	0	−6.78	−22.66	−22.51	−28.61
7	40	−5.85	−24.34	−21.01	−29.53	**26**	0	−5.70	−22.56	−22.97	−29.41
8	50	−6.74	−23.22	−21.30	−29.55	**27**	0	−6.63	−22.63	−22.64	−28.80
9	30	−6.59	−22.81	−23.09	−30.54	**28**	5	−6.70	−26.26	−23.15	−31.50
10	6	−6.39	−23.67	−22.30	−29.85	**29**	0	−6.72	−25.47	−22.92	−30.71
11	35	−5.66	−22.77	−22.93	−29.49	**30**	0	−7.30	−23.72	−22.06	−28.99
12	40	−6.62	−22.46	−23.74	−29.53	**31**	40	−7.80	−25.32	−24.07	−31.84
13	10	−5.57	−22.31	−22.45	−30.64	**32**	0	−6.85	−24.04	−23.72	−31.21
14	13	−7.18	−23.49	−23.39	−30.27	**33**	0	−7.35	−24.68	−23.22	−30.40
15	60	−7.13	−24.41	−23.43	−31.76	**34**	3	−7.15	−23.17	−23.26	−31.22
16	10	−7.38	−24.79	−24.78	−34.70	**35**	0	−7.53	−25.36	−25.65	−31.31
17	30	−5.32	−23.93	−23.06	−29.97	**36**	87	−6.16	−23.10	−21.54	−30.94
18	8	−5.55	−24.38	−22.91	−30.91	**37**	84	−7.30	−25.10	−24.24	−32.28
19	19	−7.20	−22.91	−23.20	−29.69	**38**	87	−8.48	−26.94	−22.60	−31.47

binding site and conformation of these compounds to design new benzimidazole derivatives as potential selective inhibitors. The considerable mobility of this enzyme [20] requires the use of techniques that consider such phenomena. Some of the most widely used approaches that account for protein flexibility [21] include the use of a residue conformer library that considers partial flexibility in the receptor, local minimization of the ligand–enzyme complex or a full minimization of these complexes by molecular dynamics. However, these techniques have disadvantages, such as the lack of proper representation of the flexibility phenomena of the system or the computational cost of the procedure [22]. Molecular dynamics have been used to study this system [23]. Unfortunately, despite current efforts to accelerate molecular dynamics simulations for the study of the ligand–protein complex phenomenon [24], the use of this method would be a time-consuming task to analyze more than 20 compounds in a short period of time.

Therefore, in this work we explore a procedure that involves flexible docking calculations that varies the definition of the binding site and a clustered analysis of the results. This procedure that would take a fraction of time of a molecular dynamic calculation could assist in accelerating the drug design process.

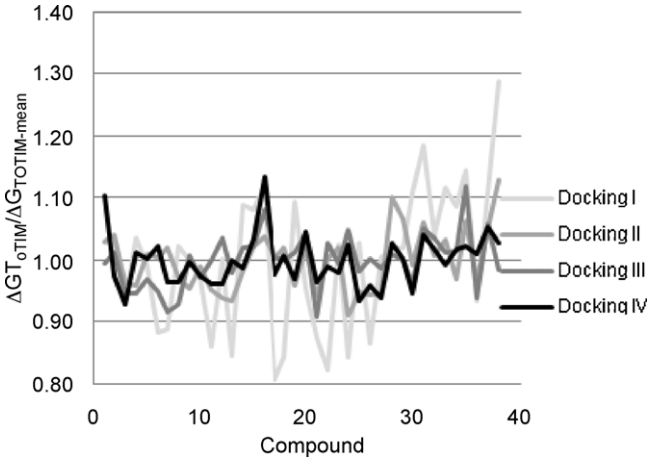

Fig. 1. Compared behavior among docking procedures.

2. Materials and methods

2.1. Computational methods

Ligands. The previously synthesized benzimidazole derivatives listed in Table 1 [17,25–29] were constructed and minimized using the semiempirical method PM6 implemented in Gaussian 09 [30]. The torsional roots and branches were indentified using MGLTools 1.5.4 [31], and Gasteiger-Marsilli atomic charges were assigned. The files were saved in the proper format for use in the Autodock4.0 system [32,33]. Compounds **A**–**G** were designed using the structure from the most active compounds from **1** to **38** as base scaffold. Then, the hybridization of these scaffolds was performed using as simple linkers amide or tioether groups. It was considered that the size of these new molecules would be enough to bind to the interface of TcTIM and reside in it completely.

Proteins. The crystallographic structure for TcTIM (PDB: 1TCD) was downloaded from the Protein Data Bank web site [34]. The

Table 4
Unclustered analysis of docking scores.

Parameter	Dockings			
	I	II	III	IV
R^2	0.2656	0.3969	0.3056	0.3742
n (for L.R.)	29	29	29	29
Slope (S.D.)	−0.19 (0.10)	−0.14 (0.06)	−0.16 (0.09)	−0.16 (0.07)
Intercept (S.D.)	−0.95 (0.68)	−3.07 (1.34)	−3.45 (1.99)	−4.61 (2.05)
Hits	11	7	9	11
Active hits	9	6	7	8
False positives	2	1	2	3
False negatives	17	20	19	18

Table 6
Docking scores of compounds **A**–**G**.

Compound	Binding energy (ΔG) (kcal/mol)			
	I	II	III	IV
A	−6.66	−24.17	−22.78	−30.38
B	−6.63	−24.39	−25.01	−30.32
C	−8.23	−25.18	−22.55	−29.48
D	−7.21	−23.70	−25.37	−25.54
E	−7.29	−24.19	−23.60	−30.17
F	−6.96	−25.17	−25.56	−27.30
G	−7.00	−23.64	−22.52	−28.39

crystallographic waters, counter-ions and ligands were removed using the Biopolymer Preparation Tool implemented on Sybyl 8.0 [35]. Subsequently, all hydrogens were added and the structure was relaxed 2000 steps using the AMBER02 force-field with a dielectric constant of 20, as reported previously [36]. Using MGLTools 1.5.4, Gasteiger-Marsilli atomic charges were assigned, and the non-polar hydrogens were fused. The files were saved in the proper format for use with both the Autogrid 4.0 and Autodock 4.0 systems.

Docking studies. The docking studies were performed using the Autodock 4.0 system. The docking procedures are listed in Table 2. The grid calculation was done with a grid size of 90 Å × 90 Å × 90 Å centered at the interface with 0.375 Å spacing. A Lamarckian genetic algorithm was used as a search method. A total of 20 runs were performed with the maximal number of energy evaluations set to 5,000,000 and initial populations of 150 conformers, the rest of the parameters were set with their default values. Initially, a "blind" docking was performed at the interface as the first ligand binding position; then, the four procedures were undertaken using the best energy result of the previous procedure as an initial conformation.

In vitro inhibition experiments. The TcTIM percentage of inhibition at a fixed concentration for each compound was determined as previously reported [37]. Briefly, recombinant TcTIM protein [38] at a concentration of 5 μg/mL was incubated at 36 °C in a buffer containing 100 mM triethanolamine, 10 mM EDTA, pH 7.4 (TE) and the compound to be tested (Table 1) dissolved in 10% of dimethyl sulfoxide (DMSO). After 2 h, 1 μL was withdrawn and added to 1 mL of reaction mixture for the activity assay. Inhibition of TcTIM activity was measured indirectly quantifying the amount of NADH consumed by the reduction of DHAP by α-glycerolphosphate dehydrogenase. None of the molecules tested here affected the activity of this enzyme used for trapping the product.

3. Results and discussion

Compounds **1**–**38** were used as a work group, while compounds **A**–**G** were used as a test group. The docking I was a procedure that considered rigid the enzyme structure and reproduced well the results obtained previously [14,15] for compounds **36**, **37** and **38**. In these works, it was found that some residues from the interface, particularly Ile69, Thr70, Tyr102 and Lys113, are important for the binding of these compounds. Despite these coincidences, the motility of the system is disregarded in this procedure; therefore, results from docking I were only considered as starting conformation for the other docking procedures which considered flexible residues for the calculation.

Four scores, calculated as estimated binding energy of the complex, were obtained corresponding to each docking procedure as listed in Table 3. The scores from docking I were significantly higher than the scores from the flexible dockings. These differences among the magnitude of the docking scores could be attributed to the Autodock algorithm, which applies to the flexible residue the same conformational search algorithm applied to the ligand, thus finding better scoring conformations of the flexible residues and the ligand than the initial conformation. To compare graphically the scores of the procedures, the docking score for each compound was divided by the mean of docking scores in each procedure and this number was plotted, as shown in Fig. 1. From this plot no clear coincidences among the docking procedures can be seen; however, a slight coincidence exists among the flexible procedures (dockings II, III and IV).

For docking III, a pocket identifier was used and implemented in SITE-ID on Sybyl. This algorithm uses a grid method for identifying possible pockets within protein structures that are relatively small, or where the solvent cannot enter easily. In this study, only 11 possible pockets in the entire enzyme were found using this algorithm, but only one pocket was large enough (34 Å^3) at the homodimeric interface formed by the residues listed in Table 2. Notably, this pocket is conformed not only by the residues of the aromatic pocket, but also by some residues that go deep into the interface of the structure.

One reason for the similarity among docking scores of II, III and IV could be the coincident residues among them. Another reason might be that the procedure for docking IV considered the same flexible residues that were considered in dockings II and III. Indeed, despite the selection of the flexible residues under different criteria, there were three coincident residues: Tyr103, Glu105 and Lys113, which are now considered important for the binding of this type of molecules. This observation is consistent with previous papers

Table 5
Clustered analysis of docking scores.

Parameter	Cluster 1				Cluster 2			
	I	II	III	IV	I	II	III	IV
R^2	0.0690	0.0541	0.1784	0.1616	0.5260	0.7205	0.2339	0.0518
n (for L.R.)	18	9	11	5	20	21	16	11
Slope (S.D.)	−0.13 (0.21)	−0.09 (0.27)	−0.10 (0.13)	−0.07 (0.22)	−0.22 (0.08)	−0.15 (0.04)	−0.10 (0.09)	−0.04 (0.10)
Intercept (S.D.)	−0.54 (1.36)	−2.01 (6.44)	−1.96 (2.96)	−1.76 (5.66)	−1.10 (0.53)	−3.36 (0.89)	−2.09 (1.91)	−0.91 (2.96)
Hits					11	12	11	18
Active hits					9	9	10	15
False positives					2	3	1	3
False negatives					17	17	16	11

Table 7
Percentage of calculated and experimental TIM inhibition.

Compound	Calculated inhibition at 100 μM								Experimental inhibition at 100 μM
	Unclustered analysis				Clustered analysis				
	I	II	III	IV	I	II	III	IV	
1	**26–42**	**30–46**	12–25	54–100	**28–43**	35–51	**18–43**	**1–74**	30
2	26–42	32–50	18–32	11–25	22–46	**2–51**	22–46	**8–38**	10
3	15–30	10–24	**0–13**	**0–10**	16–29	13–27	**0–41**	**0–70**	7
4	**27–43**	8–23	0–13	**27–43**	**22–47**	11–25	0–20	**11–43**	29
5	**22–37**	**24–38**	2–18	**24–39**	**21–42**	**28–43**	7–23	**11–41**	30
6	**7–26**	24–36	**0–13**	31–50	8–23	27–41	**0–20**	11–46	8
7	8–27	**27–41**	0–7	5–21	9–24	**31–46**	**0–42**	**0–66**	40
8	25–41	13–26	0–10	5–21	22–46	0–44	0–18	5–38	50
9	**23–38**	6–22	16–29	**21–35**	**25–39**	9–24	**14–33**	**11–40**	30
10	20–34	19–31	**3–18**	11–25	21–34	22–36	7–24	8–38	6
11	3–24	6–21	14–26	4–20	**1–40**	9–23	13–31	**5–38**	35
12	24–39	0–18	**23–42**	5–21	25–39	4–19	**25–52**	5–38	40
13	**1–23**	**0–17**	**6–20**	23–37	**2–20**	**1–17**	**9–25**	11–40	10
14	0–21	**22–35**	15–29	13–26	0–16	**26–40**	**13–33**	**0–66**	30
15	**1–23**	27–42	13–26	26–42	**0–40**	**4–41**	13–31	11–42	8
16	6–26	1–19	**0–6**	6–21	7–23	4–20	**0–17**	6–38	0
17	**0–22**	23–35	21–38	19–32	**0–17**	26–40	16–41	10–39	0
18	26–41	27–42	12–25	14–27	27–42	32–47	12–29	9–38	0
19	1–23	**0–12**	25–49	31–51	**0–40**	**0–10**	17–49	6–76	0
20	26–42	4–20	7–21	**0–11**	22–46	7–22	9–26	**0–69**	0
21	4–25	2–19	14–27	3–19	5–22	5–20	19–44	4–38	0
22	24–39	3–20	9–22	**0–13**	21–43	6–21	11–27	**0–68**	0
23	31–51	17–29	19–35	18–31	34–53	19–33	15–38	**10–38**	13
24	30–50	28–42	20–36	35–59	33–52	32–47	15–38	10–50	60
25	33–57	31–48	31–66	62–100	37–59	37–54	19–62	**0–86**	10
26	31–52	**8–23**	**17–31**	**8–23**	34–54	**11–25**	**14–35**	**6–38**	19
27	18–33	27–42	24–46	**37–64**	19–32	32–47	17–46	**9–52**	48
28	35–60	36–58	37–86	30–49	22–45	54–79	14–34	6–77	5
29	35–60	36–58	37–86	30–49	22–45	**0–67**	19–44	11–41	0
30	35–60	36–58	37–86	30–49	36–56	**0–39**	4–22	**0–39**	0
31	35–60	36–58	37–86	30–49	43–70	43–63	**26–58**	**10–51**	40
32	35–60	36–58	37–86	30–49	22–48	1–38	16–43	6–73	0
33	35–60	36–58	37–86	30–49	22–61	3–46	22–46	11–39	0
34	35–60	36–58	37–86	30–49	34–52	15–29	14–36	11–44	3
35	35–60	36–58	37–86	30–49	21–67	44–63	21–77	11–45	0
36	15–31	11–25	0–12	26–42	14–39	14–28	0–41	5–71	87
37	32–55	34–54	27–54	40–69	22–60	0–57	26–61	8–56	84
38	43–86	49–87	8–22	32–53	**51–89**	**62–91**	15–42	11–47	87
A	25–41	26–40	11–18	20–26	27–41	30–45	12–29	10–39	5[a]
B	24–40	28–43	**34–54**	19–25	26–40	**3–44**	**26–79**	10–39	52[a]
C	**43–83**	**36–58**	7–14	4–12	50–85	**43–63**	10–26	5–38	48[a]
D	32–55	20–33	36–59	0	36–56	**0–41**	20–72	0–100	20[a]
E	33–57	36–40	**22–31**	16–23	37–58	**2–41**	**16–41**	**10–38**	33[a]
F	**29–48**	36–57	38–62	0	**23–53**	43–62	**21–76**	**0–46**	34[a]
G	30–49	19–32	7–14	0	32–50	22–36	**9–26**	**0–41**	18[a]

[a] Experimental inhibition determined at 200 μM.

[14,15]. Furthermore, Tyr103 in TcTIM is replaced by Phe in HsTIM, thus providing a marker for selectivity between both enzymes.

The uncompetitive inhibition of an enzyme is a very complex phenomenon that involves several steps, the binding of the inhibitor being just one of these steps. At this moment, molecular docking is capable of predicting the affinity of certain ligand to a macromolecule, but the affinity of this ligand is not necessarily reflected in the biological response of the macromolecule, and this biological response could be a non-linear response to the concentration of the ligand. Due to these facts, it is not expected to find a quantitative correlation between the docking scores and the percentage inhibition at a fixed concentration.

Despite the poor linear correlation of the variables at hand, e.g. the docking score and the percentage inhibition at a fixed concentration, these linear correlations allowed the categorization of the results in order to analyze them in a semiquantitative way. The best linear correlation of the data were found by eliminating up to 25% of the points that decreased the linear correlation, in addition, the data that increased the linear correlation. Then, using these improved correlations the inhibition percentage for each compound in every docking procedure was calculated. According to the inhibition percentage, compounds for each docking were categorized in hits, active hits, false positives and false negatives, using the following criteria:

- A compound was considered a hit if the experimental inhibition percentage was within the confidence interval of the calculated inhibition percentage.
- A compound was considered an active hit if the compound was active within the confidence interval calculated activity.
- A compound was considered a false positive or negative if the experimental results were outside the interval of confidence of the calculated inhibition percentage.

The correlation data, as well other parameters, are listed in Tables 4 and 5.

The clustering of the docking scores was determined using the mass center coordinates for each low-energy conformation and the

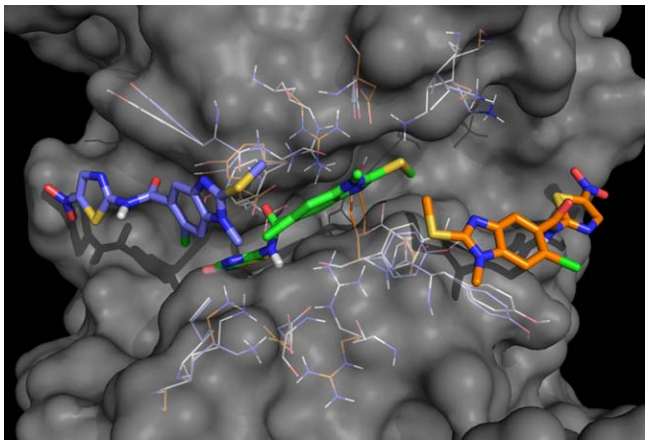

Fig. 2. Docking results of **8** with TcTIM. The rigid docking (I, green) is centered at the interface, while the flexible dockings (II, cyan and III, orange) are posed at both ends of the interface as a mirror image of the other. (For interpretation of the references to colour in this figure legend, the reader is referred to the web version of the article.)

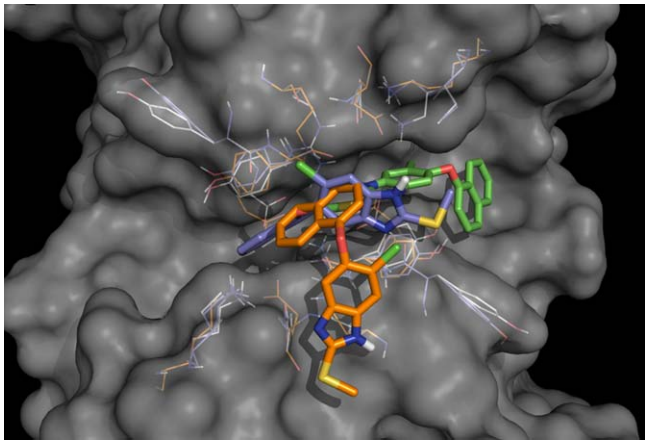

Fig. 3. Docking results of **23** with TcTIM. The rigid docking (I, green) and the flexible dockings (II, cyan and III, orange) are centered at the interface in a similar manner. Note that docking III was partially outside the interface, posing the 2-substituent of the benzimidazole nucleus towards the catalytic site. (For interpretation of the references to colour in this figure legend, the reader is referred to the web version of the article.)

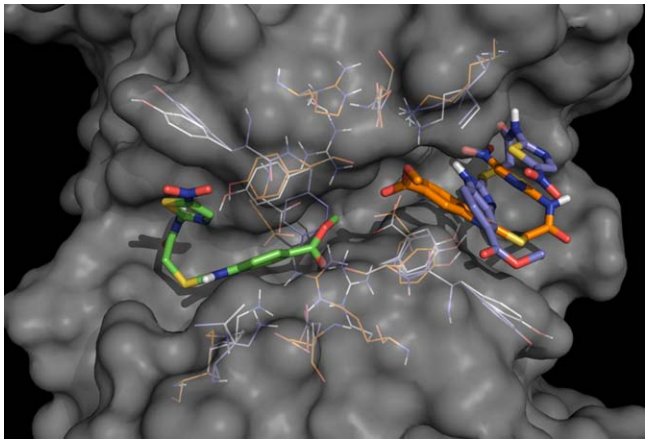

Fig. 4. Docking results of **B** with TcTIM. The rigid docking (I, green) is posed at the opposite end of the interface of the flexible dockings (II, cyan and III, orange) in a similar manner. The flexible dockings are posed in an "inverted" way with respect to each other, suggesting that there is more than one way for these molecules to bind at the same site of the interface. (For interpretation of the references to colour in this figure legend, the reader is referred to the web version of the article.)

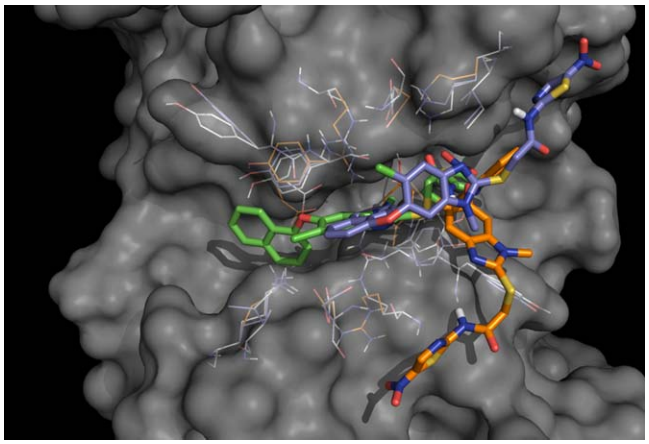

Fig. 5. Docking results of **E** with TcTIM. The rigid docking (I, green) is centered at the interface, while the flexible dockings (II, cyan and III, orange) are posed at the end of the interface. Docking III, as seen with **23** in Fig. 3, is pointed at the 2-subtituent of the benzimidazole nucleus towards the catalytic site (cavity at the bottom of the image). (For interpretation of the references to colour in this figure legend, the reader is referred to the web version of the article.)

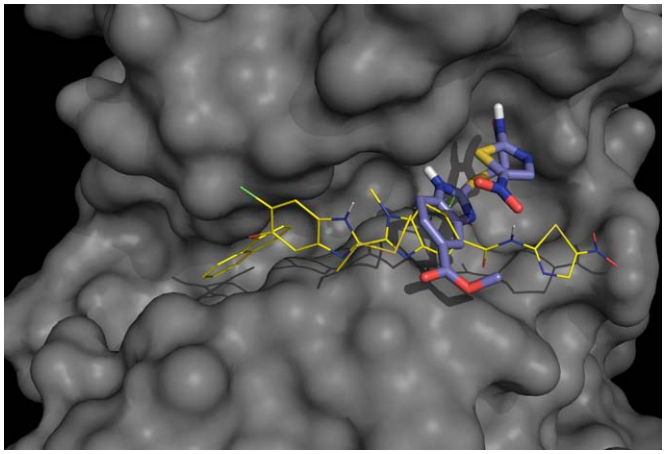

Fig. 6. Superposition of docking II results for **8**, **23** and **B**. The parent compounds **8** and **23** were docked facing each other, validating the design of **8**, which bound to the same site as its parent compounds.

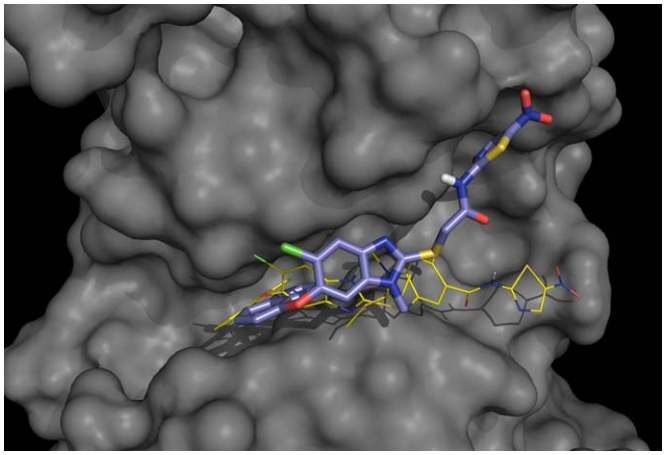

Fig. 7. Superposition of docking II results for **8**, **23** and **E**. The parent compounds **8** and **23** were docked facing each other, validating the design of E, which bound to the same site its parent compounds.

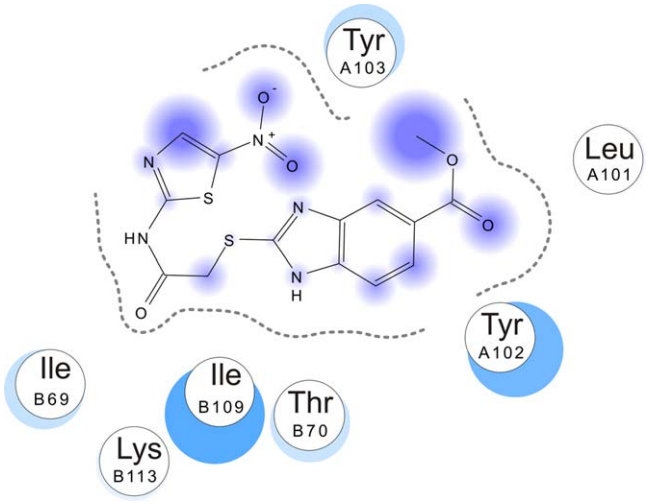

Fig. 8. Ligand interaction diagram for **B** (docking II). The dotted lines depict the ligand proximity to the residues of the enzyme, the circles show the residues at 5 Å from the ligand and the faded cyan circles show the ligand exposure to the solvent. (For interpretation of the references to colour in this figure legend, the reader is referred to the web version of the article.)

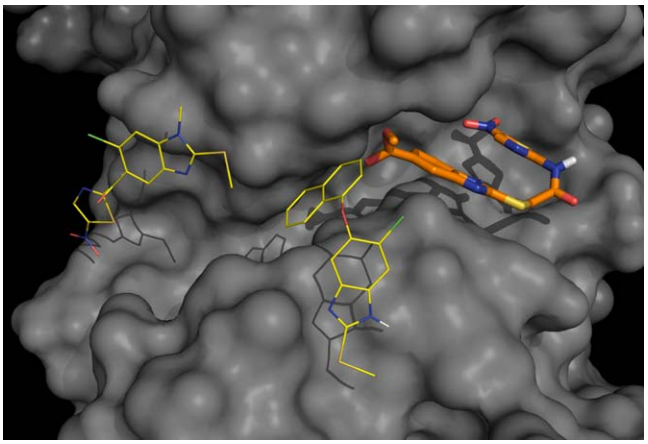

Fig. 10. Superposition of docking III results of **8**, **23** and **B**. Compound B was mirrored at the opposite end of the interface from its parent compound 8.

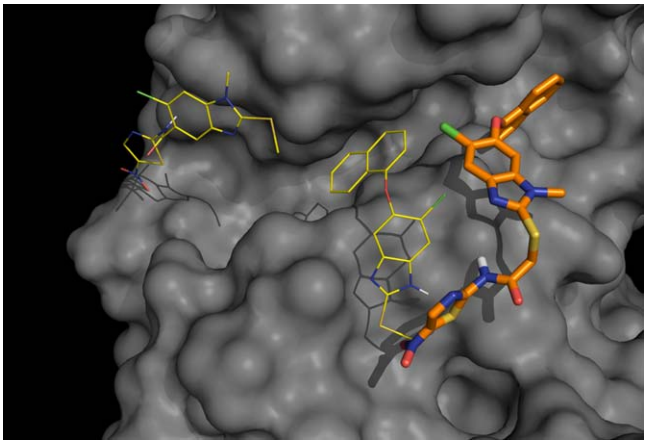

Fig. 11. Superposition of docking III results of **8**, **23** and **E**. Compound **E** was mirrored at the opposite end of the interface from its parent compound **8**. The 2-subtituent of the benzimidazole nucleus is pointed towards the catalytic site (cavity at the bottom of the image) in the same way as the parent compound **23**.

corners' coordinates of the calculation grid. The relative position of each compound mass center was determined and the Euclidean distances to these points were calculated. These results allowed clustering the conformations which had the minimal distance to the same corner. Subsequently, the mass center of each cluster was calculated as the average of the mass center position of all cluster members. From this procedure two clusters were determined; the first (cluster 1) was smaller than the other one (cluster 2) in all docking procedures. The more residues that were considered as flexible, the more clusters were dispersed, as is manifested in the linear regression parameters from cluster 2 of docking IV. The unexpected dispersion of the clusters could be explained by the methodology followed by the Autodock algorithm. Naturally, the more residues that were considered as flexible, the more conformations with good scoring are possible.

As shown in Tables 4 and 5, analyses with unclustered and clustered dockings are different. From the numerical point of view, the unclustered analyzes show a tendency between the number of flexible residues and the correlation factor; the most correlated being the docking II and IV. Taking into account the clustering, both dockings I and II provided the best results. It is seen a correlation between the score and the percentage of inhibition, therefore giving a closer view of the binding site of compounds **1**–**38**. Notably, the linear regression analysis for docking IV is the worst of the docking procedures, despite having the highest number of hits and the

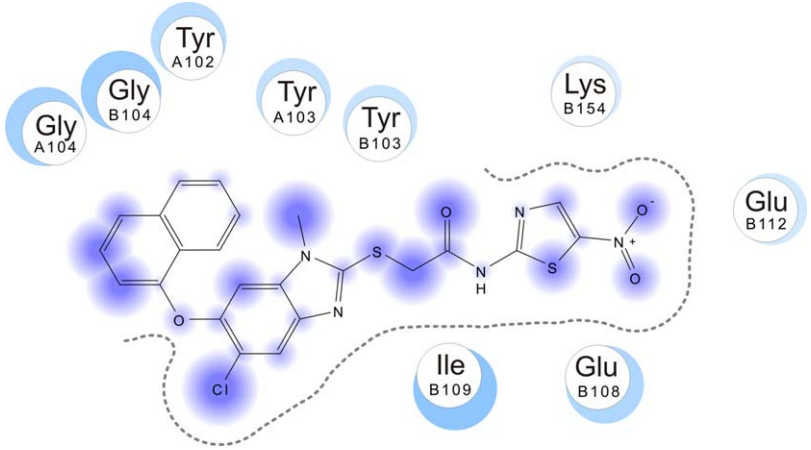

Fig. 9. Ligand interaction diagram for **E** (docking II). The dotted lines depict the ligand proximity to the residues of the enzyme, the circles show the residues at 5 Å from the ligand and the faded cyan circles show the ligand exposure to the solvent. (For interpretation of the references to colour in this figure legend, the reader is referred to the web version of the article.)

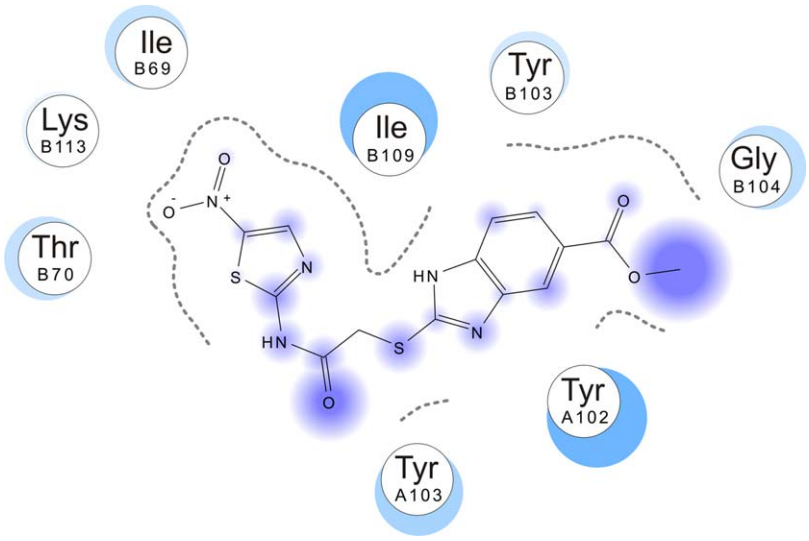

Fig. 12. Ligand interaction diagram for **B** (docking III). The dotted lines depict the ligand proximity to the residues of the enzyme, the circles show the residues at 5 Å from the ligand and the faded cyan circles show the ligand exposure to the solvent. (For interpretation of the references to colour in this figure legend, the reader is referred to the web version of the article.)

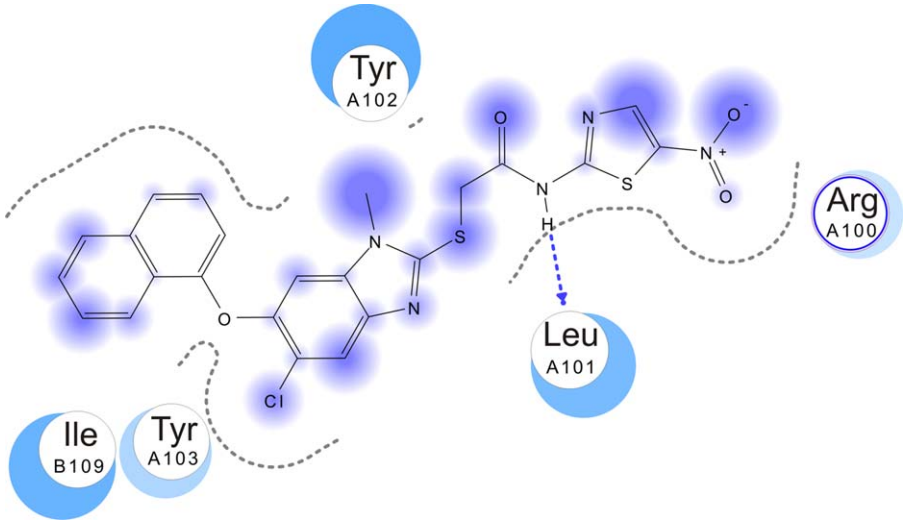

Fig. 13. Ligand interaction diagram for **E** (docking III). The dotted lines depict the ligand proximity to the residues of the enzyme, the circles show the residues at 5 Å from the ligand, and the faded cyan circles show the ligand exposure to the solvent. The arrow shows the possible hydrogen bonds between the ligand and the protein. (For interpretation of the references to colour in this figure legend, the reader is referred to the web version of the article.)

lowest number of false negatives (18 and 11 respectively); these numbers are a consequence of the linear regression itself, because the hits, active hits, false positives and false negatives were calculated from the confidence interval of the linear regression. As expected, a poor correlation between docking scores and experimental inhibition provided a broad confidence interval.

The docking results for compounds **A**–**G** are presented in Table 6 and the inhibition percentage calculated for each compound is listed in Table 7.

As observed for compounds **1**–**38**, the calculated inhibition using unclustered analysis for compounds **A**–**G** is not consistent with the experimental results, highlighting the importance of the clustering analysis. Indeed, the calculated inhibition with the clustered results, as seen in the linear regression analysis, is more consistent with the experimental results (Table 7 in bold). Within these results, dockings II and III provide the best docking results as compared with the experimental values.

Once the best dockings (II and III) were identified, the ligand–enzyme complexes of the lead candidates for the design of compounds **A**–**G** (compounds **8** and **23**) and the best compounds form the test group **B** and **E** were analyzed. A general view of complexes TcTIM-**8**, TcTIM-**23**, TcTIM-**B** and TcTIM-**E** is shown in Figs. 2–5. The flexible residues are depicted as lines.

It is seen in Figs. 2–5 that the interface forms a binding pocket across the homodimeric enzyme. The rigid docking (I, green) gives conformations that fit deep within the interface of the enzyme. In contrast, the flexible docking (II, cyan and III, orange) tends to give conformations that are partially outside the interface. These conformations fit at both ends of the interface. Therefore, clustering the results for these procedures is needed. The selection of the flexible residues is greatly affected if the low-energy conformation tends to remain in the binding pocket or partially outside. Despite having 3 residues in common, docking III gave results that are partially outside of the interface as compared with docking II, thus suggesting that the residues from docking II are more suitable to be considered as flexible for this type of ligand.

Compounds **A**–**G**, designed from the hybridization of the common scaffold of **1**–**22** and **23**–**27**, were assumed that when

united could produce better ligands for TcTIM. The complex enzyme–ligand analysis gives insight into the fitness of this design, as shown in Figs. 6 and 7 for **B** and **E**, the best inhibitors of the test group. For docking II, the design hypothesis for **B** and **E** is valid because the low-energy conformation (cyan sticks, Figs. 6 and 7) are partially superposed (compound **B**, Fig. 6) or fully superposed (compound **E**, Fig. 7) to the low-energy conformations of the parent compounds **8** and **23** (yellow lines, Figs. 6 and 7); **B** and **E** have almost the same binding site as the parent compounds. The ligand interaction diagrams for compounds **B** and **E** [39] are shown in Figs. 8 and 9, respectively.

As seen in Figs. 8 and 9, compounds **B** and **E** have a great part of their surfaces exposed to the solvent (blue circles), but they also interact with relevant residues such as Ile69, Thr70, Leu101, Tyr102, Tyr103, Ile109, Glu122 and Lys154, which are different in HsTIM (Val68, Thr69, His100, Val101, Phe102, Leu108, Gln121 and Asn153 respectively). This observation provides more information for the future design of selective inhibitors.

In the case of docking III shown in Figs. 10 and 11, the design hypothesis can be neither validated nor rejected, because the low-energy conformation of **8** is in another cluster at the other end of the interface with respect to both **B** and **E** (yellow lines at the left, Figs. 10 and 11). However, due to the enzyme's symmetry, the binding site of **8** could be considered as the mirror image of the binding site of **B** and **E** at the interface. Compound **E**, was docked in a similar way to **23**, extending part of the molecule outside of the interface which in **E** is formed by a 5-nitro-2-aminothiazolyl moiety.

The ligand interaction diagrams for docking III of **B** and **E** are shown in Figs. 12 and 13. Both compounds have a great part of their surfaces exposed to the solvent (blue circles), but also interact with relevant residues such as Ile69, Thr70, Leu101, Tyr102, Tyr103 and Ile109, which are different in HsTIM (Val68, Thr69, His100, Val101, Phe102 and Leu108 respectively). This observation provides more information for the future design of selective inhibitors. For compound **E**, there is also a hydrogen bond to the peptide chain from Leu101A that anchors the nitrothiazolyl moiety towards the vicinity of the active site.

Considering that compounds **B** and **E** were designed from compounds **8** and **23**, that the activity of the designed compounds was similar to that of the parent compounds, and that compound **8** was the most active of them all, suggest that the scaffold of **8** is the main responsible for the activity of these hybrid compounds. No additive effect could be seen in these experiments.

Finally, conformations from docking III of **23** and **E** have a hydrophobic aromatic moiety interacting with the interface and a polar moiety near the active site (the cavity at the bottom of Fig. 9). These conformations suggest that, due to the amphiphilic nature of **23** and **E**, these molecules could bind to the hydrophobic pocket of the interface, and also prevent DHAP from entering the catalytic site, as a possible mechanism of action. Naturally, more studies are needed to verify this hypothesis.

4. Conclusions

A series of docking procedures to study *T. cruzi* triosephosphate isomerase experimental inhibition by new benzimidazole derivatives are presented. It was possible to propose a flexible docking procedure, with a clustered analysis, that reproduces experimental inhibition results moderately well, identifying the residues Ile69, Thr70, Leu101, Tyr102, Tyr103, Glu105, Ile109 and Lys113 within the enzyme's interface as a possible target for further optimization of selective inhibitors. Moreover, a possible mechanism of action was proposed for future research.

Acknowledgements

The authors acknowledge the Mexican National Council of Science and Technology (CONACyT) for financing project 80093. Antonio Romo-Mancillas is very grateful to CONACyT for the graduate scholarship 173861. The authors also thank to Dr. José Luis Medina-Franco and Dr. Fabián López-Vallejo from Torrey Pines Institute for Molecular Studies at Port St. Lucie, Fl. (U.S.) for the critical evaluation of this manuscript and helpful suggestions for this paper.

References

[1] F. Guhl, J.K. Lazdins-Helds, Chagas disease report , in: Special Program for Research and Training in Tropical Diseases, World Heald Organization, Buenos Aires, Argentina, 2007.
[2] J.A. Urbina, Chemotherapy of Chagas disease , Current Pharmaceutical Design 8 (4) (2002) 287–295.
[3] F. Lakhdar-Ghazal, C. Blonski, M. Willson, P. Michels, J. Perie, Glycolysis and proteases as targets for the design of new anti-trypanosome drugs , Current Topics in Medicinal Chemistry 2 (5) (2002) 439–456.
[4] Paul A.M. Michels, F.R. Opperdoes, P.A.M. Michels, Enzymes of carbohydrate metabolism as potential drug targets , International Journal for Parasitology 31 (5–6) (2001) 482–490.
[5] V. Zomosa-Signoret, et al., Crosstalk between the subunits of the homodimeric enzyme triosephosphate isomerase , Proteins 67 (1) (2007) 75–83.
[6] E. Maldonado, et al., Differences in the intersubunit contacts in triosephosphate isomerase fromm two closely related pathogenic trypanosomes , Journal of Molecular Biology 283 (1) (1998) 193–203.
[7] R. Pérez-Monfort, et al., Derivatization of the interface cysteine of triosephosphate isomerase from *Trypanosoma brucei* and *Trypanosoma cruzi* as probe of the interrelationship between the catalytic sites and the dimer interface , Biochemistry 38 (13) (1999) 4114–4120.
[8] V. Olivares-Illana, et al., Structural differences in triosephosphate isomerase from different species and discovery of a multitrypanosomatid inhibitor , Biochemistry 45 (8) (2006) 2556–2560.
[9] J. Gayosso-De-Lucio, et al., Selective inactivation of triosephosphate isomerase from *Trypanosoma cruzi* by brevifolin carboxylate derivatives isolated from Geranium bellum Rose , Bioorganic & Medicinal Chemistry Letters 19 (20) (2009) 5936–5939.
[10] G. Álvarez, et al., Massive screening yields novel and selective *Trypanosoma cruzi* triosephosphate isomerase dimer-interface-irreversible inhibitors with anti-trypanosomal activity , European Journal of Medicinal Chemistry 45 (12) (2010) 5767–5772.
[11] A. Téllez-Valencia, et al., Highly specific inactivation of triosephosphate isomerase from *Trypanosoma cruzi* , Biochemical and Biophysical Research Communications 295 (4) (2002) 958–963.
[12] A. Téllez-Valencia, et al., Inactivation of triosephosphate isomerase from *Trypanosoma cruzi* by an agent that perturbs its dimer interface , Journal of Molecular Biology 341 (5) (2004) 1355–1365.
[13] L.M. Espinoza-Fonseca, J.G. Trujillo-Ferrara, Exploring the possible binding sites at the interface of triosephosphate isomerase dimer as a potential target for anti-tripanosomal drug design , Bioorganic & Medicinal Chemistry Letters 12 (2004) 3141–3154.
[14] L.M. Espinoza-Fonseca, J.G. Trujillo-Ferrara, Structural considerations for the rational design of selective anti-trypanosomal agents: the role of the aromatic clusters at the interface of triosephosphate isomerase dimer , Biochemical and Biophysical Research Communications 328 (4) (2005) 922–928.
[15] L.M. Espinoza-Fonseca, J.G. Trujillo-Ferrara, Toward a rational design of selective multitrypanosomatid inhibitors: a computational docking study , Bioorganic & Medicinal Chemistry Letters 16 (24) (2006) 6288–6292.
[16] R. Chávez-Calvillo, J. Miguel Costas, Hernández-Trujillo, Theoretical analysis of intermolecular interactions of selected residues of triosephosphate isomerase from *Trypanosoma cruzi* with its inhibitor 3-(2-benzothiazolylthio)-1-propanesulfonic acid , Physical Chemistry Chemical Physics 12 (9) (2010) 2067–2074.
[17] G. Navarrete-Vázquez, et al., Synthesis and antiparasitic activity of 2-(trifluoromethyl)-benzimidazole derivatives , Bioorganic & Medicinal Chemsitry Letters 11 (2) (2001) 187–190.
[18] J. Valdez, et al., Synthesis and antiparasitic activity of 1H-benzimidazole derivatives , Bioorganic & Medicinal Chemistry Letters 12 (16) (2002) 2221–2224.
[19] D. Valdez-Padilla, et al., Synthesis and antiprotozoal activity of novel 1-methylbenzimidazole derivatives , Bioorganic & Medicinal Chemistry 17 (4) (2009) 1724–1730.
[20] S. Rozovsky, A.E. McDermott, The time scale of the catalytic loop motion in triosephosphate isomerase , Journal of Molecular Biology 310 (1) (2001) 259–270.
[21] M. Trotov, R. Abagyan, Flexible ligand docking to multiple receptor conformations: a practical alternative , Current Opinion in Structural biology 18 (2) (2008) 174–184.
[22] C. B-Rao, J. Subramanian, S.D. Sharma, Managing protein flexibility in docking and its applications , Drug Discovery Today 14 (7–8) (2009) 394–400.

[23] N. Díaz-Vergara, A. Piñeiro, Molecular dynamics study of triosephosphate isoemrase from *Trypanosoma cruzi* in water/decane mixtures , Journal of Physical Chemistry B 112 (11) (2008) 3529–3539.
[24] J.D. Durrant, J.A. McCammon, Computer-aided drug-discovery techniques that account for receptor flexibility , Current Opinion in Pharmacology 10 (6) (2010) 770–774.
[25] A. Hernández-Campos, F. Ibarra-Velarde, Y. Vera-Montenegro, N. Rivera-Fernández, R. Castillo, Synthesis and fasciolicidal activity of 5-cloro-2-methylthio-6-(1-naphthyloxy)-1H-benzimidazole , Chemical & Pharmaceutical Bulletin 50 (5) (2002) 649–652.
[26] M. Reyes, et al., Paramphistomicidal efficacy of an experimental compound in sheep , Parasitology Research 102 (4) (2008) 705–708.
[27] O. Soria-Arteche, et al., Síntesis y actividad antiparasitaria de nuevos híbridos de nitazoxanida y derivados bencimidazólicos , in: XLIV Congreso Mexicano de Química, Puebla, Pue., Mexico, September, 2009, p. 143.
[28] R. Castillo, et al., "síntesis de 2-(1H-bencimidazoil-2-iltio)-N-1,3-tiazol-2-ilacetamidas sustituidas como potenciales inhibidores de la triosafosfato isoemrasa de *Trypanosoma cruzi* , in: XLIV Congreso Mexicano de Química, Puebla, Pue., Mexico, September, 2009, p. 86.
[29] I. Velázquez-Martínez, et al., Design, synthesis, and biological activity of novel hybrids of benzimidazole and 5-nitrofurfural hydrazone , in: 239th American Chemical Society National Meeting, San Francisco, CA, USA, March, 2010, pp. MEDI-449.
[30] Gaussian Inc., Gaussian09, 2009, Wallingford, CT.
[31] M.F. Sanner, Python: a programming languaje for software untegration and development , Journal of Molecular Graphics and Modelling 17 (1) (1999) 57–61.
[32] G.M. Morris, et al., Automated docking using a Lamarckian genetic algorithm and an empirical binding free energy function , Journal of Computational Chemistry 19 (14) (1998) 1639–1662.
[33] R. Huey, G.M. Morris, A.J. Olson, D.S. Goodsell, A semiempirical free energy force field with charge-based desolvation , Journal of Computational Chemistry 28 (6) (2007) 1145–1152.
[34] H.M. Berman et al., The Protein Data Bank, 2000, RCSB PDB www.pdb.org.
[35] Tripoc Inc., Sybyl 8.0, 2001, St. Louis, MO.
[36] I.T. Christensen, F.S. Jorgensen, Molecular mechanics calculations of proteins. Comparison of different enery minimization strategies , Journal of Biomolecular Structure & Dynamics 15 (3) (1997) 473–488.
[37] A. Gómez-Puyou, et al., Using evolutionary changes to achieve species-specific inhibition of enzyme action—studies with triosephosphate isomerase , Chemistry & Biology 2 (12) (1995) 847–855.
[38] P. Ostoa-Saloma, et al., Cloning, expression, purification and caracterization of triosephosphate isomerase from *Trypanosoma cruzi* , European Journal of Biochemistry 224 (3) (1997) 700–705.
[39] A.C. Wallace, R.A. Laskowski, J.M. Thornton, LIGPLOT: a program to generate schematic diagrams of protein–ligand interactions , Protein Engineering 8 (2) (1995) 127–134.